

## Detailed Description of the Conformation and Location of Membrane-Bound Erythromycin A Using Isotropic Bicelles

Nobuaki Matsumori,\* Atsushi Morooka, and Michio Murata

Department of Chemistry, Graduate School of Science, Osaka University, 1-16 Machikaneyama, Toyonaka, Osaka 560-0043, Japan

Received December 1, 2005

Although many nonpeptidic drugs target biological membrane and membrane proteins, it is still difficult to define the membrane-bound structure of the drugs. In this study, we utilized bicelles as a membrane model, since the bicelles, which have planar lipid bilayer portions, are thought to be a more appropriate and practical membrane model than micelles. Bicelles with a small diameter allow for measurements of liquid NMR due to fast tumbling in solution. We targeted erythromycin A (EA) as a membrane-binding compound because it is pointed out that the drug interacts with lysosomal membranes, inhibits phospholipase A, and consequently induces phospholipidosis as a side effect. The conformation of EA in the bicelle was successfully determined on the basis of coupling constants and NOEs. Measurements of intermolecular NOEs and paramagnetic relaxation times revealed that the drug is located shallowly in the membrane surface, with the dimethylamino group being close to the phosphate, and the macrolide portion adjacent to upper sides of the acyl chains. This study shows the general utility of isotropic bicelles for detailed conformational and orientational studies of membrane-associated nonpeptidic drugs.

### Introduction

In recent decades, it has become increasingly clear that knowledge of drug–membrane interactions is essential for the understanding of drug activity, selectivity, and toxicity.<sup>1</sup> To analyze the interactions, exploration of the membrane-bound structures of drugs is indispensable. Sodium dodecyl sulfate (SDS) or other amphiphilic surfactant micellar media have been frequently used in NMR studies to mimic the membrane environment,<sup>2–4</sup> even though serious concerns regarding the small radius of curvature and the lack of true bilayer structures arise. Recently, it has been shown that phospholipid bicelles provide more natural membrane environments, since they have planar lipid bilayer portions.<sup>5,6</sup> The bicelles generally consist of a long-chain phospholipid, most commonly dimyristoylphosphatidylcholine (DMPC), and a short-chain one such as dihexanoylphosphatidylcholine (DHPC). Their size and shape are controlled by the ratio,  $q$ , of long-chain phospholipids to short ones. At high  $q$  ratios ( $>2.5$ ), the bicelles adopt a magnetically aligned  $\alpha$ -lamellar bilayer morphology like sliced Swiss cheese.<sup>7–12</sup> Alternatively, with a decrease in the  $q$  values, the aggregate becomes disk-shaped,<sup>13–17</sup> where the bilayer region formed by the long-chain lipid is surrounded by a rim consisting of the short-chain lipid. The discoidal shape of bicelles is retained even at  $q$  values smaller than 1.<sup>15–17</sup> The small and isotropic bicelles permit high-resolution NMR measurements in solution and, therefore, begin to be used for structural determinations of membrane-associated peptides.<sup>18–24</sup> The greatest merit for the use of isotropic bicelles over micelles is that the bicelle interior consists of a true lipid bilayer. Indeed, the small size and high curvature of micelles can not only induce conformational strain in attached peptides<sup>6</sup> but also cause peptides to take different positions.<sup>18</sup>

Despite these ideal membrane mimetic properties of the isotropic bicelle, its application is mostly limited to small membrane-associated peptides, and the isotropic bicelle has not been fully explored as a membrane model for nonpeptidic

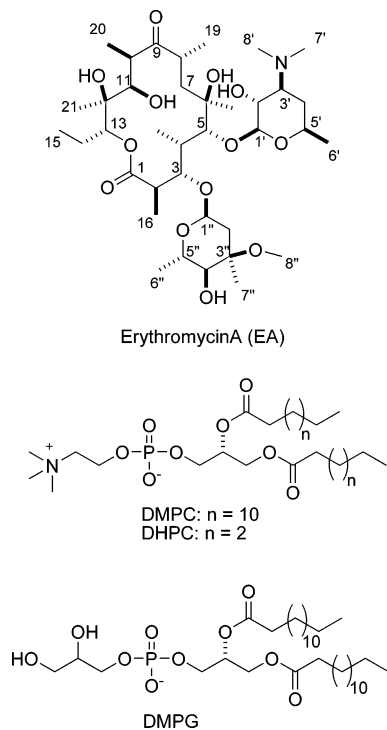
membrane-acting drugs except for cannabinoids.<sup>25</sup> Hence, the aim of this study is to seek the general utility of fast-tumbling bicelle media toward the determination of the conformation and location of membrane-associated nonpeptidic molecules. Among various membrane-acting organic compounds, we have first chosen erythromycin A (EA), a widely prescribed macrolide antibiotic, because, although its site of action is the bacterial ribosome, the drug and its analogues are known to accumulate in lysosomal membranes and potentially induce phospholipidosis as a side effect (Chart 1).<sup>26,27</sup> Phospholipidosis-inducing drugs bind principally to negatively charged lysosomal membranes and inhibit lysosomal phospholipase activity, resulting in the accumulation of undigested phospholipids within the organelle.<sup>27</sup> Since phospholipidosis is a significant clinical concern, further molecular characterization of the interactions between drugs and phospholipids is needed for a comprehensive understanding of the toxicity. Therefore, the determination of the membrane-bound structure of EA, a representative macrolide antibiotic, is clinically significant.

In this paper, we report the conformation and location of EA in fast-tumbling bicelles ( $q = 0.5$ ) and also discuss the possible mechanism of the phospholipase inhibition of EA and its analogues in biological membranes.

### Results and Discussion

Since EA is known to accumulate in acidic lysosomal membranes, the bicelle containing dimyristoylphosphatidylglycerol (DMPG) at 10 mol % of DMPC was used in this study. The drug was incorporated into the isotropic bicelle ( $q = 0.5$ ) at 8 mol % of total phospholipids to facilitate the observation of NMR signals of EA. To examine whether the bicelle structure is maintained in the presence of highly contained EA, we first measured <sup>31</sup>P NMR spectra of a large oriented bicelle ( $q = 3.3$ ) containing EA at 18.6 mol % of total phospholipids. In oriented bicelles with the normal perpendicular to the direction of the magnetic field, <sup>31</sup>P NMR spectra show two well-resolved resonances: the high-field resonance is attributed to the long-chain DMPC in the planar section, whereas the downfield resonance is attributed to the short-chain DHPC on the edges

\* To whom correspondence should be addressed. Phone: (81) 6 6850 5569. Fax: (81) 6 6850 5569. E-mail: matumori@ch.wani.osaka-u.ac.jp.

**Chart 1.** Structures of EA and Phospholipids Used in This Study

of the disks or covering the Swiss cheese perforations.<sup>28</sup> An increase in the magnitude of the isotropic  $^{31}\text{P}$  NMR signal generally indicates membrane lysis by a drug, since the lysis results in an increased amount of small fast tumbling phospholipid structures such as mixed micelles. Hence,  $^{31}\text{P}$  NMR is useful in probing the effect of a drug on the morphology of bicelles. The resultant  $^{31}\text{P}$  spectrum observed for the oriented bicelle containing EA was typical of well-aligned bicelles and was almost identical to what was observed without EA (Figure 1). Although the minute  $^{31}\text{P}$  chemical shift difference in the presence and absence of EA may indicate that EA slightly weakens the orientation of aligned bicelles, this result totally shows that EA does not act as a detergent destroying bicelle structure, thus confirming the applicability of the bicellar system to the following structural study of EA.

Then we measured conventional one- and two-dimensional NMR spectra of EA with  $q = 0.5$  bicelles comprised of deuterated phospholipids (DMPC- $d_{54}$ , DHPC- $d_{22}$ , and DMPG- $d_{54}$ ). As described above, it is known that the discoidal shape of bicelle is retained even at  $q$  values smaller than 1.<sup>15–17</sup> DQF-COSY and TOCSY spectra were utilized to fully assign the proton resonances of EA (Table 1). Since the chemical shifts of 3'- and 7',8'-protons in  $\text{CDCl}_3$  are reported to be 2.43 and 2.29 ppm, respectively,<sup>29</sup> the low-field-shifted resonances of these protons listed in Table 1 indicate that the dimethylamino group is protonated in the bicelle.

The conformation of EA associated with the isotropic bicelle was determined on the basis of NOE and  $^3J_{\text{HH}}$  data obtained from NOESY and DQF-COSY, respectively. NOE peak intensities were divided into three groups with upper distance limits of 3.0, 4.0, and 5.0 Å (Table 1). To derive dihedral angles from  $^3J_{\text{HH}}$  values, we utilized a modified Karplus equation that takes into account the effects of electronegative functional groups<sup>30</sup> (Table 2). The total numbers of interproton distance and dihedral restraints derived from the NMR data were 46 and 6, respectively. On the basis of these conformational constraints, molecular modeling was performed using Monte Carlo coupled

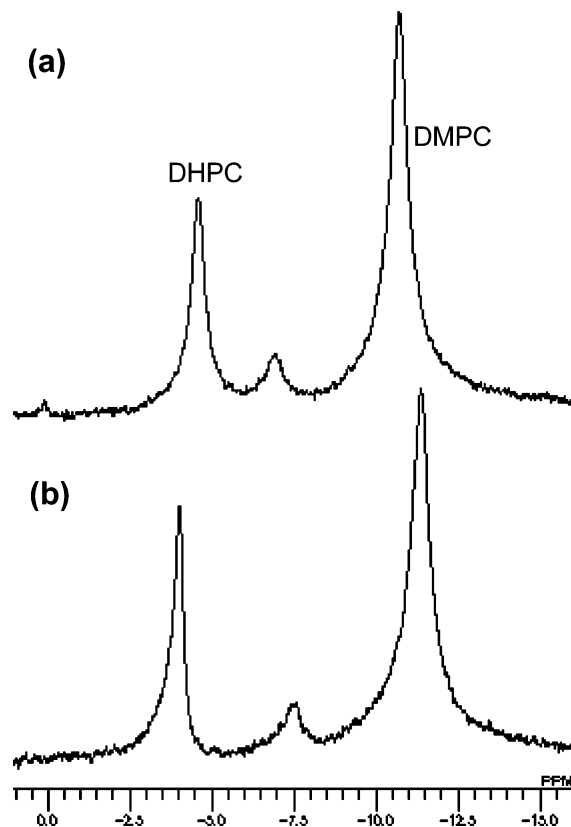


**Figure 1.**  $^{31}\text{P}$  NMR spectra of oriented bicelles ( $q = 3.3$ ) containing EA at 18.6 mol % of total phospholipids (a) and without EA (b). The high-field resonance is attributed to the long-chain DMPC in the planar section whereas the downfield resonance to the short-chain DHPC on the edges. These spectra are typical of magnetically oriented bicelles and almost identical to each other, implying that the bicelle morphology is not destroyed by the inclusion of EA.

with a low-mode conformation search algorithm<sup>31</sup> available in Macro-Model version 8.5.<sup>32</sup>

Figure 2 shows a superposition of the 12 lowest-energy conformations of EA in isotropic bicelles within 1 kcal/mol. The macrocyclic lactone portion of the drug appears highly ordered, and positions of the two sugar moieties relative to the lactone ring also converge well. This conformation excellently agrees with the crystal structure of EA.<sup>33</sup> Extreme values of the vicinal coupling constants in the lactone ring (Table 2) indicate that motional averaging in the lactone ring barely occurs, which is consistent with the highly ordered conformation of the lactone as shown in Figure 2.

Similarly, we determined the conformation of EA in SDS micelles. However, there was no major difference in the conformation of EA between bicelles and micelles (Figure 2 and Table 2). This may reflect the stable and rigid conformation of EA. We never think that this result negates the utility of bicelle systems, since we have recently found that an ionophore antibiotic adopts different conformations under micellar and bicellar environments (manuscript in preparation), which probably results from the morphological difference between bicelles and micelles. Furthermore, bicelles having planar bilayer regions are evidently more appropriate for positioning studies of drugs in a lipid bilayer, as demonstrated below.

Paramagnetic ions (i.e.,  $\text{Mn}^{2+}$ ,  $\text{Gd}^{3+}$ , and  $\text{Dy}^{3+}$ ) and nitroxyl spin-labels have long been used in determining the depth of bound entities in micelles and lipid vesicles. A paramagnetic agent enhances the relaxation of NMR nuclei in the vicinity of the paramagnetic center. For example, relaxation induced by

**Table 1.**  $^1\text{H}$  Chemical Shifts of EA in a  $q = 0.5$  Bicelle (HOD at 4.65 ppm) and NOE Data

position <sup>a</sup>	$\delta_{\text{H}}$	NOEs <sup>b</sup>	position <sup>a</sup>	$\delta_{\text{H}}$	NOEs <sup>b</sup>
2	2.91	4(m), 16(m), 17(s)	1'	4.62	3'(m), 5'(s), 5''(s)
3	3.89	4(w), 5(s), 16(w), 1''(s)	2'	3.49	4'h(w), 7',8'(s)
4	2.01	7l(w), 11(s), 17(m)	3'	3.43	4'l(m), 7',8'(s)
5	3.57	18(s), 1'(s), 6'(m), 5''(s)	4'h	1.53	7',8'(s)
7h	1.63	11(w)	4'l	2.11	5'(w), 6'(m), 7',8'(s)
7l	1.87	11(m)	5'	3.85	6'(s)
8	2.8	18(s), 19	6'	1.29	
10	3.21		7',8'	2.84	
11	3.84	13(s), 21(s)	1''	4.93	2''h(w), 2''l(m), 5''(s)
13	5.08	14h(w), 14l(w), 15(s)	2''h	1.68	
14h	1.49	15(w)	2''l	2.41	7''(s), 8''(m)
14l	1.90	15(m)	4''	3.21	
15	0.85		5''	4.13	6''(s), 7''(m)
16	1.20	1''(s)	6''	1.31	
17	1.09	1'(s)	7''	1.25	8''(s)
18	1.39		8''	3.32	
19	1.20				
20	1.13				
21	1.17				

<sup>a</sup> h, high-field resonance; l, low-field resonance. <sup>b</sup> The NOE connectivities are listed once according to the proton having the lower number. The intensity of NOEs is represented in parentheses as strong (s), medium (m), or weak (w).

**Table 2.**  $^3J_{\text{HH}}$  Values of EA in Isotropic Bicelles and SDS Micelles

bond	$^3J_{\text{HH}}$ in bicelles (Hz)	dihedral angle <sup>a</sup> (deg)	$^3J_{\text{HH}}$ in micelles (Hz)
H2–H3	9.3	146	8.7
H3–H4	1.3	–98	1.2
H4–H5	9.6	150	7.0
H7h–H8	2.3	–67	1.8
H7l–H8	11.9	168	10.4
H10–H11	<1.0	75	0.8
H13–H14h	11.4	–177	11.1
H13–H14l	1.0	73	1.2

<sup>a</sup> Dihedral angle constraints deduced from the modified Karplus relation.<sup>30</sup>

$\text{Mn}^{2+}$  has been frequently used to estimate nuclei exposed to the aqueous exterior of membranes.<sup>18,34,35</sup> Likewise, 5-doxy and 12-doxy phospholipids were used to detect NMR nuclei in the hydrophobic interior of membranes.<sup>18</sup> Both were used in this study to determine which protons were exposed to the water–lipid interface and which were confined to the hydrophobic interior of the bicelle.

The paramagnetic contribution to the spin–lattice relaxation is best represented by  $T_{1\text{M}}$

$$\frac{1}{T_{1\text{M}}} = \frac{1}{T_{1\text{P}}} - \frac{1}{T_1^0}$$

where  $T_1^0$  is the spin–lattice relaxation time in the absence of paramagnetic agents and  $T_{1\text{P}}$  that in their presence.<sup>36</sup> Paramagnetic relaxation time  $T_{1\text{M}}$  has explicit  $r^6$  distance dependency, which makes it possible to measure semiquantitatively the depth of membrane-bound entities. To examine the location of  $\text{Mn}^{2+}$  and 1-palmitoyl-2-stearoyl-5(12)-doxyl-*sn*-glycero-3-phosphocholine (5/12-doxy PSPC) in the bicelle, we first measured the paramagnetic effects of these agents on  $T_1$  relaxation times of protons of bicelle phospholipids. The results are shown in Figure 3.  $\text{Mn}^{2+}$  ions effectively enhanced the relaxation of protons close

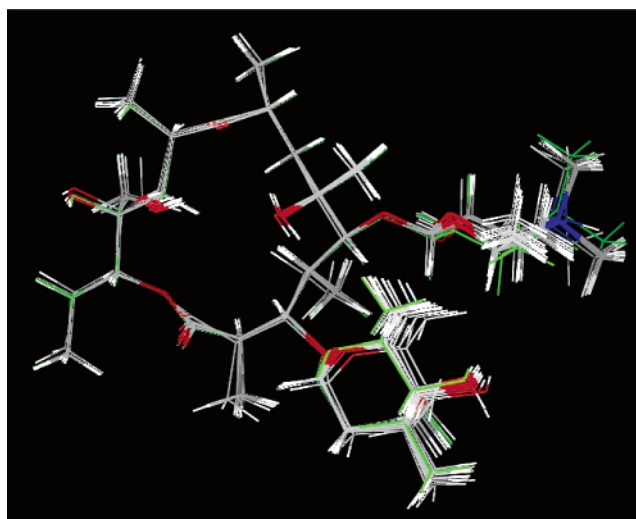


**Figure 2.** Ensemble of the 12 lowest-energy conformations of EA within 1 kcal/mol in an isotropic bicelle ( $q = 0.5$ ). The calculation was performed with the MCMC-Low-Mode method using the MMFF force field based on NOE and  $^3J_{\text{HH}}$  constraints. The rmsd was 0.196 Å. The green conformation is the lowest EA conformation in SDS micelle obtained in the same way.

to the phosphate group (Figure 3A), indicating that  $\text{Mn}^{2+}$  ions are preferentially situated close to the phosphate group of phospholipids. 5-Doxy-PSPC most strongly affects signals originating from the upper carbons of acyl chains (Figure 3B), while the distribution of the radical moiety of 12-doxy-PSPC gradually decreases from the chain terminus to the surface (Figure 3C). The location of each paramagnetic probe in the bicelle is schematically depicted in Figure 4. It should be emphasized that the distribution profiles of these paramagnetic probes in bicelles agree well with those in large lipid vesicles such as liposomes.<sup>35,37</sup> This indicates that these probes are properly located in the bicelle.  $T_{1\text{M}}$  values of lipid protons were unchanged in the presence and absence of EA, which again indicates that EA does not significantly perturb the conformation of bicelle phospholipids.

Then we measured  $T_{1\text{M}}$  values of EA protons in bicelles containing paramagnetic agents (Figure 5), though all the  $T_{1\text{M}}$  values could not be obtained due to overlapping signals on one-dimensional NMR. Apparently,  $\text{Mn}^{2+}$  ions most strongly influence the 7',8'-dimethylamino group, whereas other protons of EA are only weakly relaxed by  $\text{Mn}^{2+}$  (Figure 5A). The  $T_{1\text{M}}$  of 7',8'-protons is roughly comparable with that of trimethylammonium of the phospholipid, thus indicating that the dimethylamino group of EA is situated in the water–lipid interface. Since the dimethylamino group of EA is protonated in the bicelle as described above, the protonated amine is considered to have an ionic association with phosphate groups of the bicelle.

The protons most significantly affected by 12-doxy-PSPC are at positions 2, 13, 20, and 1'' (Figure 5C), suggesting the deeper immersion of these protons into the bicelle interior. Interestingly, similar paramagnetic relaxation profiles were observed between 5- and 12-doxy-PSPCs (Figure 5B). As shown in Figure 3B, the influence of 5-doxy-PSPC has its maximum at the upper carbons of phospholipid acyl chains. Therefore, the similar relaxation effects of both doxy-PSPCs on EA suggest that the entire EA molecule is predominantly localized above the upper region of phospholipid acyl chains.

The orientation of EA was further confirmed by intermolecular NOEs between EA and phospholipid, effectively measured using gradient-enhanced nuclear Overhauser effect spec-

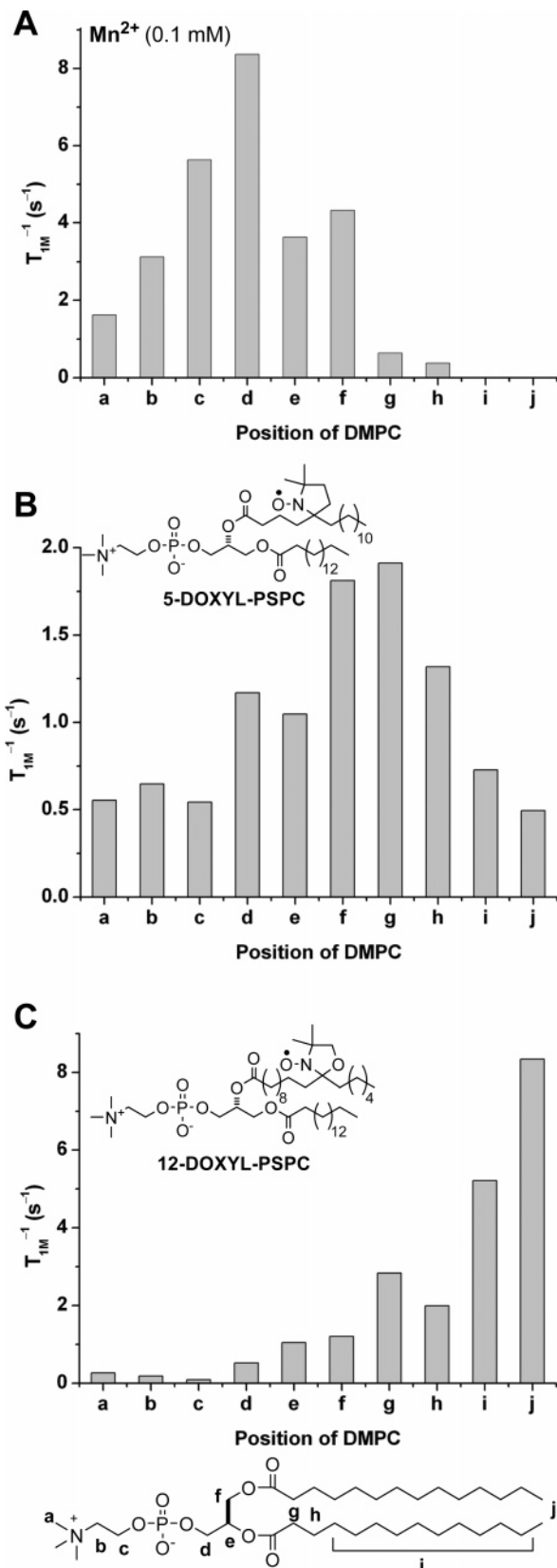


**Figure 3.** Effects of paramagnetic agents on DMPC protons in the isotropic bicelles containing EA.  $T_{1M}$  denotes the paramagnetic contribution to the spin–lattice relaxation time for proton resonances. The panels depict the inverse of  $T_{1M}$  in the presence of 100  $\mu M$   $Mn^{2+}$  (A) or 5/12-doxyI-PSPC at 1 mol % with respect to the total phospholipids (B and C).

troscopy (GOESY) experiments.<sup>38</sup> In NOE difference experiments, imperfect subtraction often gives rise to a subtraction artifact

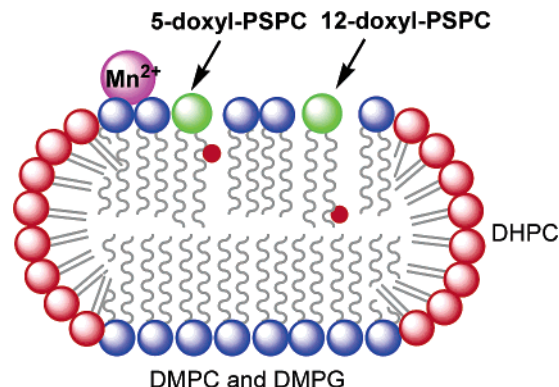


**Figure 4.** Schematic model of the location of each paramagnetic agent in the isotropic bicelle deduced from the  $T_{1M}$  values.

which makes it difficult to visualize small NOE enhancements. The GOESY method prevents the need to compute difference spectra and thus gives spectra containing no subtraction artifact, which means that much smaller NOEs can be reliably measured. Accordingly, the GOESY experiment is suitable for detection of weak intermolecular NOEs between phospholipids and EA. Selective irradiation at 7',8'-protons of EA gave distinct NOE enhancements of protons in the phospholipid polar region (Figure 6). These NOEs suggest that the dimethylamino group of EA resides in the polar region of phospholipids. Another GOESY experiment with irradiation at H-13 of EA gave a NOE only at methylene protons of the phospholipid acyl chain (data not shown), indicating that H-13 of EA is situated in the bicelle interior. These NOE data further support the results of the aforementioned paramagnetic relaxation experiments.

Then, we examined whether EA binds to the flat membrane-like area on the bicelle, since the flat area is validated as a bilayer model. For this purpose, we utilized the intermolecular NOE between trimethylammonium protons of the phospholipid and dimethylamino protons of EA. Figure 7 shows NOE enhancements at trimethylammonium protons of the bicelle phospholipid, observed by the GOESY experiment via irradiation of the dimethylamino protons of EA. The bicelle was composed of DMPC and DHPC or DMPC- $d_{13}$  (deuterated at choline protons) and DHPC. Much weaker NOE intensity in the DMPC- $d_{13}$  bicelle means that the intermolecular NOE stems not from choline protons of DHPC but mainly from those of DMPC. This manifests that EA is dominantly distributed in the DMPC-rich flat domain of the bicelle. As inferred from the formation of ionic interaction between EA and phospholipids, EA probably interacts more preferentially with acidic DMPG than with neutral DMPC or DHPC. Considering the hydrophobic matching of acyl chain lengths, DMPG is most likely located in the DMPC-rich bilayer-like region of the bicelle. It is, therefore, reasonable that EA prefers to reside in the bilayer-like area of the bicelle.

The paramagnetic experiments and intermolecular NOE measurements mentioned above show that EA is shallowly immersed in the membrane, with the dimethylamino group being located close to the phosphate group and with the macrolide portion being situated proximal to the upper sides of acyl chains. Taking this position with the conformation of EA determined above, we have developed a model structure of EA in membranes as shown in Figure 8. To provide an indication of the location of EA in the bicelle, the figure also illustrates the structural formula of the DMPC headgroup, which is depicted so that it is almost equivalent to the reported conformation of phospholipids in liquid–crystalline bilayers.<sup>39,40</sup>

Phospholipidosis induced by drugs bearing a cationic amphiphilic structure often occurs in humans and animals, which

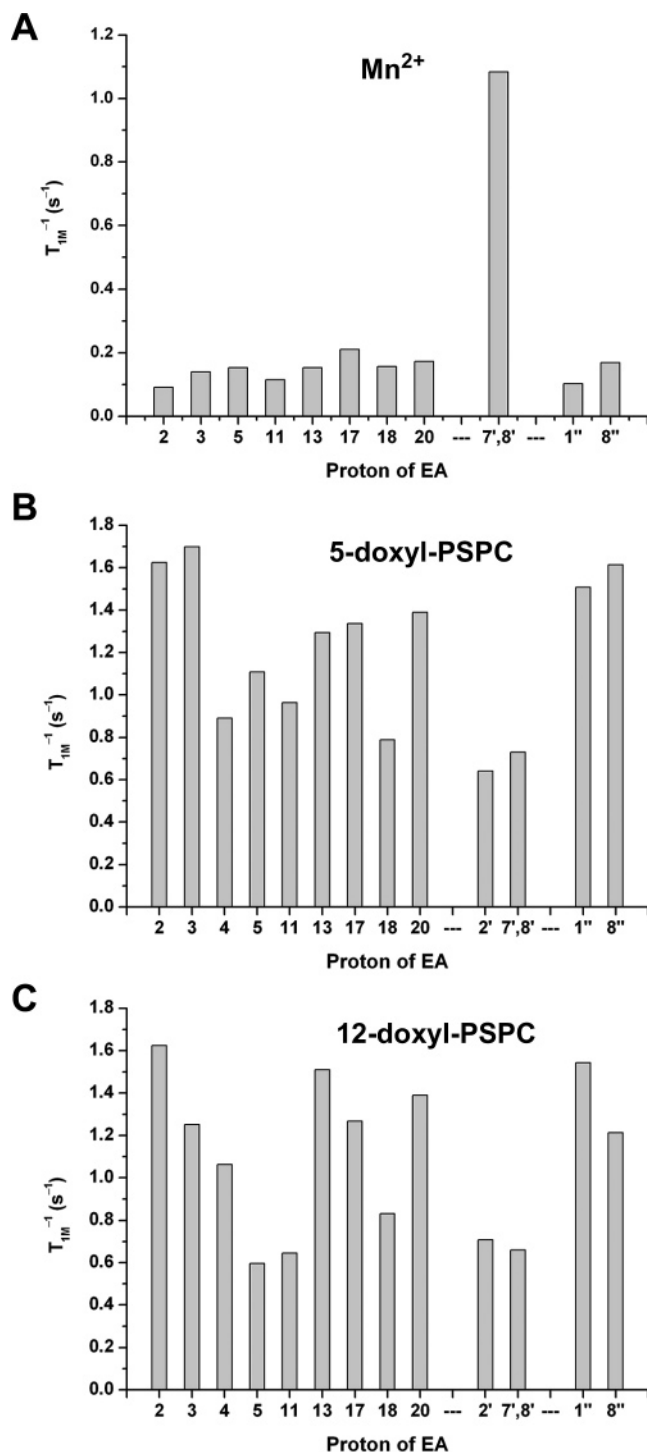


**Figure 5.** Effects of paramagnetic agents on protons of EA in isotropic bicelles. The panels depict the inverse of  $T_{1M}$  in the presence of 100  $\mu$ M Mn<sup>2+</sup> (A) or 5/12-doxy-PSPC at 1 mol % with respect to the total phospholipids (B and C).

is characterized by an intracellular accumulation of phospholipids and the concurrent development of concentric lamellar bodies.<sup>27</sup> The primary mechanism responsible for the development of phospholipidosis is binding of the drugs to negatively charged lysosomal membranes followed by an inhibition of lysosomal phospholipase activity by the drugs.<sup>27</sup> There are two or more theories for how phospholipidosis occurs. The first involves the binding of drugs to hydrophobic and hydrophilic moieties of phospholipids, resulting in complexes that cannot be digested by lysosomal phospholipases.<sup>41</sup> The second theory involves direct inhibition of lysosomal phospholipases by the

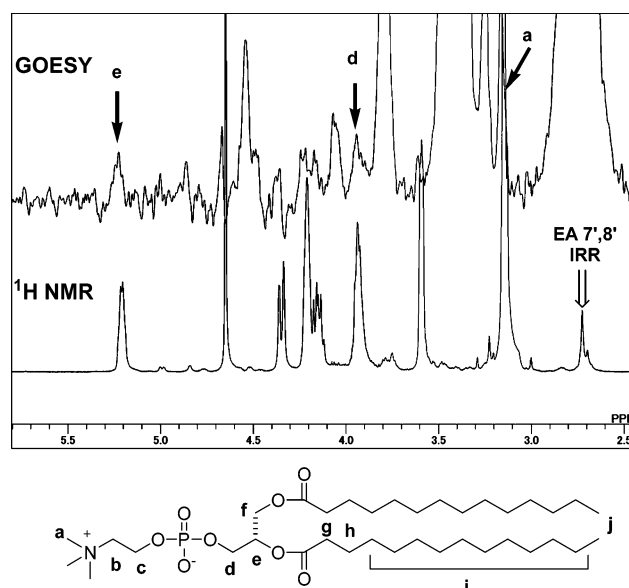


**Figure 6.** One-dimensional GOESY spectrum of an isotropic bicelle containing EA (top) and a conventional <sup>1</sup>H NMR spectrum (bottom). In the GOESY spectrum, a selective pulse was applied to 7',8'-protons of EA, and the mixing time was set to 1000 ms. Weak intermolecular NOEs were successfully observed at protons a, d, and e of phospholipids. These NOEs support the notion that the dimethylamino group of EA resides in the polar region of phospholipids. Other enhancements are assigned to intramolecular NOEs.

drugs.<sup>42</sup> In the case of phospholipidic tricyclic antidepressants, the possibility that the drugs modify the interaction between bilayer and membrane proteins by changing lipid conformation and dynamics was also reported.<sup>43</sup> It is pointed out that EA and its related drugs are also potential inducers of phospholipidosis.<sup>26</sup> Azithromycin, a derivative of EA, was suggested to attenuate the activities of lysosomal phospholipases by neutralizing the surface negative charges required by the enzymes for optimal activity.<sup>26</sup> The study presented here reveals that the bulky macrolide ring of EA resides just around the ester groups of phospholipids (Figure 8), which may allow us to propose a possible mechanism for the phospholipidosis induced by EA: the arrangement of EA in lipid bilayers sterically hinders lysosomal phospholipases from hydrolyzing the esters of phospholipids, and consequently, undigested phospholipids accumulate in the cell. Indeed, we have obtained preliminary results which show that the hydrolysis of bicellar phospholipids by phospholipase A<sub>2</sub> is delayed in the presence of EA. The mechanisms underlying phospholipidosis are not exactly the same for each phospholipidogenic drug, and therefore, this approach may be useful in identifying the mechanism of general phospholipidosis-inducing drugs.

## Conclusion

In this study, we have successfully determined the structure and location of EA bound to the membrane using the isotropic bicelle system. Since EA was shown to reside in the bilayer portion of the bicelle, it is reasonable to consider that the structure and orientation of EA obtained here substantially reproduce those in biological membranes. These techniques can be extended to a wide variety of organic molecules that interact strongly with the membranes. In fact, we have already applied this method to representative ionophore antibiotics and successfully elucidated the mechanism underlying ion transport across membranes by the drugs (manuscript in preparation). The application range of this technique is not restricted to drug-

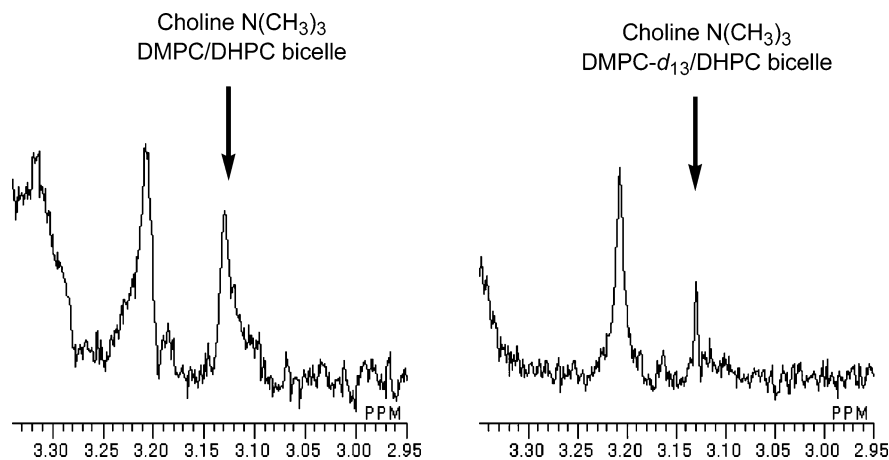


**Figure 7.** NOE enhancement at trimethylammonium protons of bicelle phospholipids measured by GOESY experiments irradiating 7',8'-protons of EA. The bicelle is composed of DMPC and DHPC (left) or DMPC-*d*<sub>13</sub> (deuterated at choline protons) and DHPC (right). The mixing time was set to 1000 ms. The apparent reduction in the NOE intensity of the DMPC-*d*<sub>13</sub> bicelle suggests the preferential localization of EA in the DMPC-rich planar region of the bicelle.

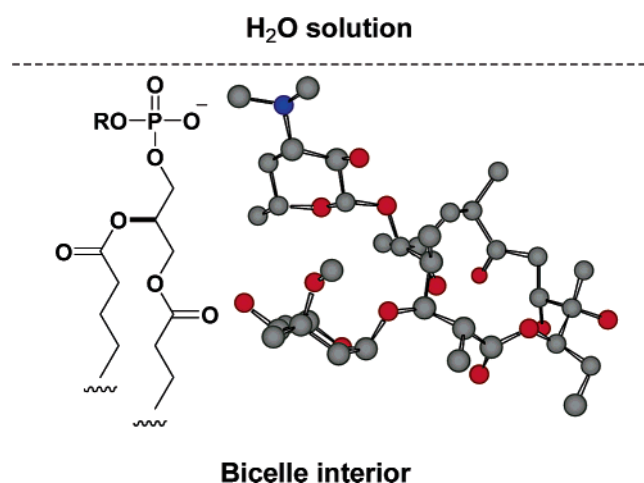


**Figure 8.** Model representing the position and conformation of EA with respect to bicelle lipid bilayers. The molecular formula of the phospholipid polar region, which is depicted as being almost equivalent to the conformation in the liquid-crystalline bilayer,<sup>39,40</sup> is also shown to provide an indication of the location of EA.

membrane interactions but can be potentially extended to interaction analyses between drugs and membrane proteins and/or peptides, which are main problems confronting modern medicinal chemistry.

### Experimental Section

**Materials.** Erythromycin A (EA) was obtained from Sigma-Aldrich and used without further purification. Normal and deuterated phospholipids, dimyristoyl-*sn*-glycerophosphatidylcholine (DMPC), DMPC-*d*<sub>54</sub>, DMPC-*d*<sub>13</sub>, dimyristoyl-*sn*-glycerophosphatidylglycerol (DMPG), DMPG-*d*<sub>54</sub>, dihexanoyl-*sn*-glycerophosphatidylcholine (DHPC), DHPC-*d*<sub>22</sub>, and the spin-labeled phospholipids 1-palmitoyl-2-stearoyl-*sn*-glycero-5-doxy-3-phosphatidylcholine (5-doxy-PSPC) and 1-palmitoyl-2-stearoyl-*sn*-glycero-12-doxy-3-phosphatidylcholine (12-doxy-PSPC) were purchased from Avanti Polar Lipids (Alabaster, AL). MnCl<sub>2</sub> was purchased from Nacalai tesque (Kyoto, Japan) and D<sub>2</sub>O from Euriso-Top. Perdeuterated sodium dodecyl sulfate (SDS-*d*<sub>25</sub>) was from Cambridge Isotope Laboratories, Inc. (Andover, MA). Other chemicals were from standard commercial sources and used without further purification.

**Sample Preparations.** For two-dimensional NMR measurements, DMPC-*d*<sub>54</sub> (5.32 mg, 7.27 μmol), DMPG-*d*<sub>54</sub> (0.60 mg, 0.81 μmol), DHPC-*d*<sub>22</sub> (7.68 mg, 16.14 μmol), and EA (1.42 mg, 1.94 μmol) were dissolved in 3 mL of CHCl<sub>3</sub>, in which the molar ratio

of phospholipids was 9:1:20 [ $q = ([\text{DMPC}] + [\text{DMPG}])/[\text{DHPC}] = 0.5$ ]. The solution was evaporated to a thin film in a flask. After the solution had been dried in vacuo for more than 8 h, D<sub>2</sub>O (170 μL) was added to the flask to give a sample with a total lipid concentration of 8% (w/v). The resultant mixture was vortexed until a clear solution was obtained and transferred to a Shigemi 5 mm NMR tube (Shigemi Inc., Tokyo, Japan). The final concentration of EA was 11 mM, and the resultant pH was around 5.5.

A sample used for one-dimensional gradient-enhanced nuclear Overhauser effect spectroscopy (GOESY) measurements was prepared in a similar manner, except that DMPC and DMPG instead of deuterated ones were used to observe intermolecular NOEs between EA and phospholipids. For experiments depicted in Figure 7, DHPC, DMPG, and DMPC or DMPC-*d*<sub>13</sub> (deuterated at choline protons) were used.

In <sup>31</sup>P NMR measurements of oriented bicelles, DMPC, DMPG, DHPC, and EA were mixed at a molar ratio of 30:3:10:8 ( $q = 3.3$ ). The final lipid concentration in D<sub>2</sub>O was set to 15% (w/v).

**NMR Spectroscopy.** NMR spectra were recorded on JEOL GSX 500 (500 MHz) and JEOL Lambda 500 (500 MHz) spectrometers. All experiments were carried out at 37 °C. Homonuclear two-dimensional experiments (DQF-COSY, NOESY, and TOCSY) were carried out in phase-sensitive mode using the States method with a 1.5 s recovery time. The number of data points was 2048 in the  $F_2$  dimension and 256 in the  $F_1$  dimension for NOESY and TOCSY and 4K ( $F_2$ ) × 128 ( $F_1$ ) for DQF-COSY. The spectral width in both dimensions was typically 3000 Hz. The data were processed using Alice2 version 4.1 (JEOL DATUM) and apodized with shifted square sine-bell window functions in both  $F_1$  and  $F_2$  dimensions. The DQF-COSY data were zero-filled in the  $F_2$  dimension to an 8K ( $F_2$ ) × 128 ( $F_1$ ) real data matrix to obtain coupling constants. NOESY spectra were recorded with mixing times of 150 and 300 ms. TOCSY spectra were recorded with a mixing time of 80 ms. In all the two-dimensional spectra, DANTE water presaturation was used to eliminate the residual water signal. Chemical shifts were referenced to the solvent chemical shift (HOD at 4.65 ppm).

<sup>31</sup>P NMR spectra were recorded on a JEOL GSX-500 spectrometer (<sup>31</sup>P at 202.35 MHz) with <sup>1</sup>H-broad band decoupling. H<sub>3</sub>PO<sub>4</sub> was used for an external chemical shift reference as 0 ppm.

One-dimensional gradient-enhanced nuclear Overhauser effect spectroscopy (GOESY) measurements were performed on a JEOL Lambda 500 MHz spectrometer equipped with a 5 mm z-gradient probe for pulsed field gradient capability. Spectra were measured at 27 °C with a spectral width of 4500 Hz and 8K data points. The recycle time between scans was 4.2 s. The measurements were performed with a constant mixing time of 1000 ms and 3000 scans, and the selective 90 and 180° pulses had durations of 15 and 30 ms, respectively. The strengths of four gradient pulses with a width of 1 ms were 5, -5, 5, and 10 G/cm in this order.

**Structure Calculations.** All the interproton distance restraints between non-*J*-coupled protons were derived from the two-dimensional NOESY experiments with a mixing time of 150 ms. Forty-six distance restraints were divided into three categories according to the NOESY cross-peak intensities. Upper bounds were fixed at 3.0, 4.0, and 5.0 Å for strong, medium, and weak correlations, respectively. Lower bounds of all distance constraints were fixed at 1.8 Å, which corresponds to twice the hydrogen van der Waals radius. Pseudoatom corrections of the upper bounds were applied for distance restraints involving the unresolved methyl protons (+1 Å). For stereospecifically assigned diastereotopic methylene protons, the interproton distances were applied to each proton according to the NOE peak intensity. A total of eight H–C–C–H dihedral angles obtained from  $^3J_{\text{HH}}$  coupling constants were used as restraints with a  $\pm 15^\circ$  allowance. These dihedral angles were obtained using the modified Karplus dihedral equation which takes into account the effects of electronegativity of relevant functional groups.<sup>30</sup>

Conformations were calculated using MacroModel version 8.5 installed on RedHat Linux 8 OS. Initial atomic coordinate and structure files were manually generated step by step. To this structure was first applied simulated annealing from 1000 to 100 K with 100 K intervals. At each temperature, MD was run during the equilibrium time of 40 ps with the NMR-based restraints. After simulated annealing, the sampling of the conformational space was performed following the Monte Carlo Multiple Minimum combined with Low-Mode method (MCMM/Low-mode).<sup>31</sup> The MMFF force field installed in MacroModel was used for the calculations. The experimental distance and dihedral restraints were represented as a soft asymptotic potential. One thousand steps of MCMM/Low-Mode were performed.

**Positioning Study.** For Mn<sup>2+</sup> relaxation experiments, a D<sub>2</sub>O solution of MnCl<sub>2</sub> was added to the bicelle solution to yield a final concentration of 100 μM MnCl<sub>2</sub>. For the experiments with spin-labeled phospholipids, either 5-doxyl-PSPC or 12-doxyl-PSPC was premixed with phospholipids and EA in CHCl<sub>3</sub> at a molar ratio of 1% with respect to the total phospholipids. The subsequent procedures were the same as the aforementioned bicelle preparation. Spin–lattice relaxation times (*T*<sub>1</sub>) were determined using a standard 180–τ–90 inversion recovery pulse sequence with 10 τ values between 0.1 and 12 s. Measurements were performed at 37 °C for the samples with and without paramagnetic probes.

**Conformation of EA in SDS Micelles.** A sample for the conformational study of EA in SDS micelles was prepared by dissolving a mixture of 0.91 mg of EA (1.24 μmol) and 12.0 mg of SDS-*d*<sub>25</sub> (38.3 μmol) in 0.60 mL of D<sub>2</sub>O. The concentrations of EA and SDS-*d*<sub>25</sub> were 2.0 and 64 mM, respectively. NMR measurements and conformational calculations were performed in the same manner that was used for the bicelle sample.

**Acknowledgment.** We are grateful to Prof. Tohru Oishi in our laboratory for invaluable discussion and Mr. Seiji Adachi in our department for NMR measurements. This work was supported by Grants-In-Aid for Scientific Research on Priority Area (A) (12045235) and for Young Scientists (B) from the Ministry of Education, Sciences, Sports, Culture, and Technology, Japan, and by a grant from CREST, Japan Science and Technology Corp.

**Supporting Information Available:** NMR spectra of EA in bicelles. This material is available free of charge via the Internet at <http://pubs.acs.org>.

## References

- Seydel, J. K.; Wiese, M. *Drug-Membrane Interactions*; Wiley-VCH: Weinheim, Germany, 2003; pp 1–31.
- Fernandez, C.; Wuthrich, K. NMR solution structure determination of membrane proteins reconstituted in detergent micelles. *FEBS Lett.* **2003**, *555*, 144–150.
- Mascioni, A.; Porcelli, F.; Ilangovan, U.; Ramamoorthy, A.; Veglia, G. Conformational preferences of the amylin nucleation site in SDS micelles: An NMR study. *Biopolymers* **2003**, *69*, 29–41.
- Porcelli, F.; Buck, B.; Lee, D.-K.; Hallock, K. J.; Ramamoorthy, A.; Veglia, G. Structure and orientation of pardaxin determined by NMR experiments in model membranes. *J. Biol. Chem.* **2004**, *279*, 45815–45823.
- Sanders, C. R.; Hare, B. J.; Howard, K. P.; Prestegard, J. H. Magnetically-oriented phospholipid micelles as a tool for the study of membrane-associated molecules. *Prog. Nucl. Magn. Reson. Spectrosc.* **1994**, *26*, 421–444.
- Chou, J. J.; Kaufman, J. D.; Stahl, S. J.; Wingfield, P. T.; Bax, A. Micelle-induced curvature in a water-insoluble HIV-1 Env peptide revealed by NMR dipolar coupling measurement in stretched polyacrylamide gel. *J. Am. Chem. Soc.* **2002**, *124*, 2450–2451.
- Gaemers, S.; Bax, A. Morphology of three lyotropic liquid crystalline biological NMR media studied by translational diffusion anisotropy. *J. Am. Chem. Soc.* **2001**, *123*, 12343–12352.
- Nieh, M. P.; Glinka, C. J.; Krueger, S.; Prosser, R. S.; Katsaras, J. SANS study of the structural phases of magnetically alignable lanthanide-doped phospholipid mixtures. *Langmuir* **2001**, *17*, 2629–2638.
- Sanders, C. R.; Landis, G. C. Reconstitution of membrane proteins into lipid-rich bilayered mixed micelles for NMR studies. *Biochemistry* **1995**, *34*, 4030–4040.
- Howard, K. P.; Prestegard, J. H. Conformation and dynamics of membrane-bound digalactosyl diacylglycerol. *J. Am. Chem. Soc.* **1996**, *118*, 3345–3353.
- Losonczy, J. A.; Prestegard, J. H. Nuclear magnetic resonance characterization of the myristoylated, N-terminal fragment of ADP-ribosylation factor 1 in a magnetically oriented membrane array. *Biochemistry* **1998**, *37*, 706–716.
- Sanders, C. R.; Landis, G. C. Facile Acquisition and Assignment of Oriented Sample NMR spectra for bilayer surface-associated proteins. *J. Am. Chem. Soc.* **1994**, *116*, 6470–6471.
- Lin, T. L.; Liu, C. C.; Roberts, M. F.; Chen, S. H. Structure of mixed short-chain lecithin/long-chain lecithin aggregates studied by small-angle neutron scattering. *J. Phys. Chem.* **1991**, *95*, 6020–6027.
- Vold, R. R.; Prosser, R. S. Magnetically oriented phospholipid bilayered micelles for structural studies of polypeptides. Does the ideal bicelle exist? *J. Magn. Reson., Ser. B* **1996**, *113*, 267–271.
- Glover, K. J.; Whiles, J. A.; Wu, G. H.; Yu, N. J.; Deems, R.; Struppe, J. O.; Stark, R. E.; Komives, E. A.; Vold, R. R. Structural evaluation of phospholipid bicelles for solution-state studies of membrane-associated biomolecules. *Biophys. J.* **2001**, *81*, 2163–2171.
- Luchette, P. A.; Vetman, T. N.; Prosser, R. S.; Hancock, R. E. W.; Nieh, M. P.; Glinka, C. J.; Krueger, S.; Katsaras, J. Morphology of fast-tumbling bicelles: A small angle neutron scattering and NMR study. *Biochim. Biophys. Acta* **2001**, *1513*, 83–94.
- van Dam, L.; Karlsson, G.; Edwards, K. Direct observation and characterization of DMPC/DHPC aggregates under conditions relevant for biological solution NMR. *Biochim. Biophys. Acta* **2004**, *1664*, 241–256.
- Lindberg, M.; Biverstahl, H.; Gräslund, A.; Mäler, L. Structure and positioning comparison of two variants of penetratin in two different membrane mimicking systems by NMR. *Eur. J. Biochem.* **2003**, *270*, 3055–3063.
- Vold, R. R.; Prosser, S. R.; Deese, A. J. Isotropic solutions of phospholipid bicelles: A new membrane mimetic for high-resolution NMR studies of polypeptides. *J. Biomol. NMR* **1997**, *9*, 329–335.
- Andersson, A.; Mäler, L. NMR solution structure and dynamics of motilin in isotropic phospholipid bicellar solution. *J. Biomol. NMR* **2002**, *24*, 103–112.
- Whiles, J. A.; Brasseur, R.; Glover, K. J.; Melacini, G.; Komives, E. A.; Vold, R. R. Orientation and effects of mastoparan X on phospholipid bicelles. *Biophys. J.* **2001**, *80*, 280–293.
- Bárány-Wallje, E.; Andersson, A.; Gräslund, A.; Mäler, L. NMR solution structure and position of transportin in neutral phospholipid bicelles. *FEBS Lett.* **2004**, *567*, 265–269.
- Marcotte, I.; Separovic, F.; Auger, M.; Gagne, S. M. A multidimensional <sup>1</sup>H NMR investigation of the conformation of methionine-enkephalin in fast-tumbling bicelles. *Biophys. J.* **2004**, *86*, 1587–1600.
- Glover, K. J.; Whiles, J. A.; Wood, M. J.; Melacini, G.; Komives, E. A.; Vold, R. R. Conformational dimorphism and transmembrane orientation of prion protein residues 110–136 in bicelles. *Biochemistry* **2001**, *40*, 13137–13142.
- Guo, J.; Pavlopoulos, S.; Tian, X.; Lu, D.; Nikas, S. P.; Yang, D.-P.; Makriyannis, A. Conformational study of lipophilic ligands in phospholipid model membrane systems by solution NMR. *J. Med. Chem.* **2003**, *46*, 4838–4846.
- Montenez, J. P.; Van Bambeke, F.; Piret, J.; Brasseur, R.; Tulkens, P. M.; Mingeot-Leclercq, M. P. Interactions of macrolide antibiotics (Erythromycin A, roxithromycin, erythromycylamine [Dirithromycin], and azithromycin) with phospholipids: Computer-aided conforma-

- tional analysis and studies on acellular and cell culture models. *Toxicol. Appl. Pharmacol.* **1999**, *156*, 129–140.
- (27) Reasor, M. J.; Kacew, S. Drug-induced phospholipidosis: Are there functional consequences? *Exp. Biol. Med.* **2001**, *226*, 825–830.
- (28) Marcotte, I.; Dufourc, E. J.; Ouellet, M.; Auger, M. Interaction of the neuropeptide met-enkephalin with zwitterionic and negatively charged bicelles as viewed by  $^{31}\text{P}$  and  $^2\text{H}$  solid-state NMR. *Biophys. J.* **2003**, *85*, 328–339.
- (29) Everett, J. R.; Tyler, J. W. An analysis of the proton and carbon-13 NMR spectra of erythromycin A using two-dimensional methods. *J. Chem. Soc., Perkin Trans. 1* **1985**, 2599–2603.
- (30) Haasnoot, C. A. G.; De Leeuw, F. A. A. M.; Altona, C. The relation between proton–proton NMR coupling constants and substituent electronegativities. I. An empirical generalization of the Karplus equation. *Tetrahedron* **1980**, *36*, 2783–2792.
- (31) Kolossvary, I.; Guida, W. C. Low-mode conformational search elucidated: Application to C39H80 and flexible docking of 9-deazaguanine inhibitors into PNP. *J. Comput. Chem.* **1999**, *20*, 1671–1684.
- (32) Mohamadi, F.; Richards, N. G.; Guida, W. C.; Liskamp, R.; Lipton, M.; Canfield, C.; Chang, G.; Hendrickson, T.; Still, W. C. MacroModel: An integrated software system for modeling organic and bioorganic molecules using molecular mechanics. *J. Comput. Chem.* **1990**, *11*, 440–467.
- (33) Harris, D. R.; McGeachin, S. G.; Mills, H. H. Structure and stereochemistry of erythromycin A. *Tetrahedron Lett.* **1965**, 679–685.
- (34) Tuzi, S.; Hasegawa, J.; Kawaminami, R.; Naito, A.; Saito, H. Regioselective detection of dynamic structure of transmembrane  $\alpha$ -helices as revealed from  $^{13}\text{C}$  NMR spectra of [ $3\text{-}^{13}\text{C}$ ]Ala-labeled bacteriorhodopsin in the presence of  $\text{Mn}^{2+}$  ion. *Biophys. J.* **2001**, *81*, 425–434.
- (35) Buffy, J. J.; Hong, T.; Yamaguchi, S.; Waring, A. J.; Lehrer, R. I.; Hong, M. Solid-state NMR investigation of the depth of insertion of protegrin-1 in lipid bilayers using paramagnetic  $\text{Mn}^{2+}$ . *Biophys. J.* **2003**, *85*, 2363–2373.
- (36) Villalaín, J. Location of cholesterol in model membranes by magic-angle-sample-spinning NMR. *Eur. J. Biochem.* **1996**, *241*, 583–593.
- (37) Vogel, A.; Scheidt, H. A.; Huster, D. The distribution of lipid attached spin probes in bilayers: Application to membrane protein topology. *Biophys. J.* **2003**, *85*, 1691–1701.
- (38) Stonehouse, J.; Adell, P.; Keeler, J.; Shaka, A. J. Ultrahigh-quality NOE spectra. *J. Am. Chem. Soc.* **1994**, *116*, 6037–6038.
- (39) Hong, M.; Schmidt-Rohr, K.; Zimmermann, H. Conformational constraints on the headgroup and sn-2 chain of bilayer DMPC from NMR dipolar couplings. *Biochemistry* **1996**, *35*, 8335–8341.
- (40) Bruzik, K. S.; Harwood, J. S. Conformational study of phospholipids in crystalline state and hydrated bilayers by  $^{13}\text{C}$  and  $^{31}\text{P}$  CP-MAS NMR. *J. Am. Chem. Soc.* **1997**, *119*, 6629–6637.
- (41) Lüllmann, H.; Lüllmann-Rauch, R.; Wassermann, O. Lipidosis induced by amphiphilic cationic drugs. *Biochem. Pharmacol.* **1978**, *27*, 1103–1108.
- (42) Kubo, M.; Hostetler, K. Y. Mechanism of cationic amphiphilic drug inhibition of purified lysosomal phospholipase A<sub>1</sub>. *Biochemistry* **1985**, *24*, 6515–6520.
- (43) Santos, J. S.; Lee, D.-K.; Ramamoorthy, A. Effects of antidepressants on the conformation of phospholipid headgroups studied by solid-state NMR. *Magn. Reson. Chem.* **2004**, *42*, 105–114.

JM051210V